Nanoscale

Accepted Manuscript

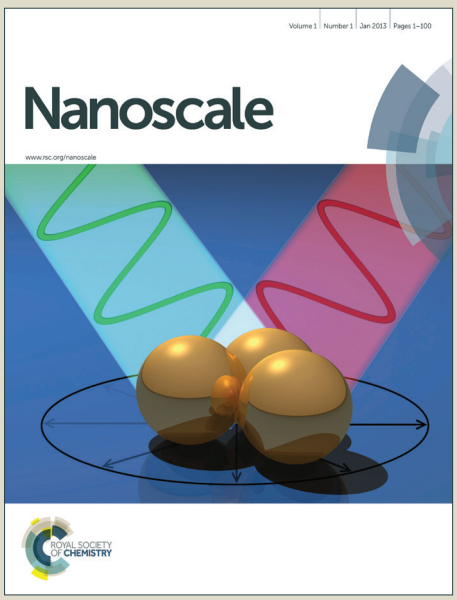

ROYAL SOCIETY OF CHEMISTRY

www.rsc.org/nanoscale

Cite this: DOI: 10.1039/c0xx00000x

www.rsc.org/xxxxxx

COMMUNICATION

Nanobursa Mesh: Graded Electrospun Nanofiber Mesh with Metal Nanoparticles on Carbon Nanotubes

Semra Senturk-Ozer,[a] Tao Chen,[a] Nebahat Degirmenbasi,[a,b] Halil Gevgilili,[a] Simon G. Podkolzin[a] and Dilhan M. Kalyon[a]*

Received (in XXX, XXX) Xth XXXXXXXXX 20XX, Accepted Xth XXXXXXXXX 20XX
DOI: 10.1039/b000000x

A new type of materials, a "nanobursa" mesh (from "bursa" meaning "sac or pouch"), is introduced. This material consists of sequential layers of porous polymeric nanofibers encapsulating carbon nanotubes, which are functionalized with different metal nanoparticles in each layer. The nanobursa mesh is fabricated via a novel combination of twin-screw extrusion and electrospinning. Use of this hybrid process at industrially-relevant rates is demonstrated by producing a nanobursa mesh with graded layers of Pd, Co, Ag, and Pt nanoparticles. Potential use of the fabricated nanobursa mesh is illustrated with modeling of catalytic hydrocarbon oxidation.

[a] *Department of Chemical Engineering and Materials Science, Stevens Institute of Technology, Hoboken, New Jersey 07030 USA; E-mail: dkalyon@stevens.edu*
[b] *Gazi University, Department of Chemistry, 06500, Teknikokullar, Ankara, Turkey*

† Electronic Supplementary Information (ESI) available: Experimental methods and computational details. See DOI: 10.1039/b000000x/

Metal nanoparticles are utilized in numerous and diverse applications, such as catalysis, sensing, environmental, separation, and biomedical fields due to their high surface to volume ratios and changes in their electronic structures compared to the respective bulk materials. Unique properties of nanoparticles make possible to formulate new materials with dramatically improved capabilities, for example, in chemical reactivity, ligand sequestration and sorption. The range of nanoparticle applications is, however, significantly hindered by their instability. The stability of nanoparticles can be improved and their range of applications, therefore, extended by anchoring them on a suitable support, such as carbon nanotubes (CNTs) or by encapsulating them into polymeric nanofibers. The range of applications can be further extended by producing materials that have tailored gradients of nanoparticles that are stable under application conditions. Electrospinning provides multiple advantages for incorporation and stabilization of various nanoinclusions, including nanotubes.[1-3] A conventional electrospinning process involves placement of a polymeric solution within a cylindrical reservoir with a plunger on one side and a needle on the other.[1, 4, 5] The plunger moves at a constant speed to force the polymer solution into the needle. The needle is attached to an electrical potential source and faces a grounded conductive surface. A whipping unstable motion is typically generated downstream to reduce the diameter of the fibers[4, 5], possibly into the nano regime. In spite of its inherent limitations, i.e., no capabilities for conveying of particulate solids, mixing, devolatilization and stripping and only limited melting and pressurization/pumping capabilities, the electrospinning process has been successfully applied to generate multiple types of ceramic, carbon and polymeric fibers and nanofibers.[1, 4] Conventional electrospinning has also been used to produce functionally graded polymeric materials, for example for biomedical applications.[6] The capabilities of electrospinning can be significantly expanded if a twin-screw extruder is used as the front-end to allow conveying and melting of solids, mixing of additives, for example nanoparticles, devolatilization, pressurization and reactive capabilities.[7] Importantly, such a hybrid process that combines a twin-screw extruder with

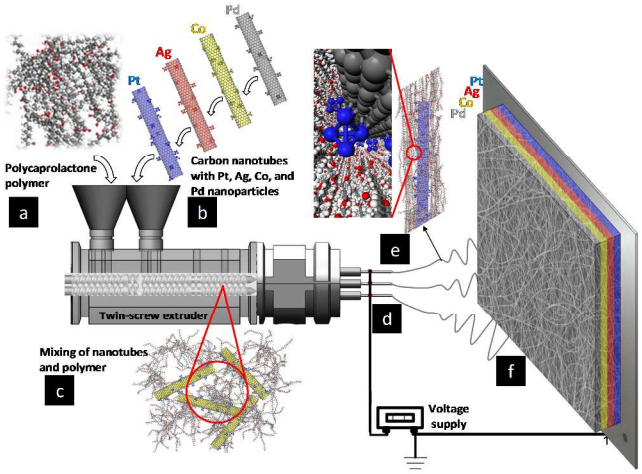

Fig. 1 Production of a graded nanofibrous mesh material (nanobursa) comprised of nanofibers encapsulating nanotubes functionalized with different types of nanoparticles with the hybrid process of twin-screw extrusion and electrospinning: Feeding of the (a) Polymer and (b) Metal-functionalized CNTs, (c) Continuous mixing of the polymer with CNTs, (d) Electrospinning via a spinneret with multiple nozzles, (e) Encapsulation of the nanotubes into polymer nanofibers, (f) Nanobursa mesh with consecutive layers of CNTs functionalized with Pd, Co, Ag, and Pt nanoparticles.

electrospinning also allows time-dependent feeding and incorporation of multiple ingredients to produce new types of nanofibrous meshes, which are graded in composition, porosity and functionality. An example of the fabrication of a new material with consecutive layers of Pd, Co, Ag, and Pt nanoparticles stabilized on multi-walled CNTs and encapsulated into a nanofibrous polymeric mesh, which is produced by time-dependent feeding, is illustrated in Figure 1. We propose to name this new type of graded nanofibrous materials a "nanobursa mesh" from "bursa", meaning "sac or pouch" (from Medieval Latin meaning "bag or purse"), to reflect their pouch-like characteristics. By stabilizing metal nanoparticles in custom-tailored gradients, nanobursa meshes introduce new capabilities for numerous applications, especially for sequential filtering, catalytic activity and simultaneous sensing of reactants and hazardous gases.

Pd, Co, Ag, and Pt nanoparticles were synthesized using wet chemistry and sonication methods.[8-11] These metal nanoparticles were selected based on current research efforts and the importance of their potential industrial applications. For example, these metal nanoparticles can be used as electrode materials for fuel cells[12] as well as in photovoltaic[13], sensing[14], hydrogen storage[15] and catalytic applications[16-19]. CNTs have been identified as a promising catalytic support in Fischer-Tropsch synthesis and numerous other catalytic chemistries.[20-23] Details of the produced nanobursa meshes are summarized in Figures 2a-g. Typical transmission electron microscope (TEM) micrographs of our functionalized nanotubes are shown in Figures 2d-g. The Pd-functionalized CNTs exhibit small Pd particles with a size of 5-8 nm as well as larger clusters with a size of up to 20 nm (Figure 2d). In contrast, the Co-functionalized CNTs exhibit only well-distributed nanoparticles with sizes less than 1 nm (Figure 2e), and the Pt nanoparticles exhibit sizes of 3-8 nm (Figure 2g). The Ag nanoparticles with sizes of 1-4 nm are imbedded into the channels of CNTs, as shown in Figure 2f. Metal nanoparticles located on the outside surface of CNTs would be more accessible in sensing and catalytic applications. On the other hand, confinement of metal nanoparticles inside CNTs has been shown to increase catalytic activity significantly despite low accessibility, for example for Rh nanoparticles in catalytic conversion of synthesis gas into ethanol.[23] Overall, our results demonstrate that all evaluated metals can be deposited on CNTs in the form of nanoparticles with excellent dispersion.

A 7.5-mm twin-screw extruder, which was specially designed to accommodate an electrospinning spinneret, was used to fabricate composition-graded nanobursa meshes by sequentially feeding nanotubes containing Pd, Co, Ag, and Pt nanoparticles into the extruder where they were dispersed into polycaprolactone (PCL), as shown in Figure 1. A multi-nozzle spinneret[24] was used to increase the fabrication rate. To allow access to the metal-functionalized CNTs for gases or liquids in sorption, catalysis and sensing applications, the nanofibers were rendered porous, as can be seen in Figure 2a. The Supporting Information section provides details on custom-tailoring the porosity by changing the type and concentration of the solvent and/or use of a porogen (Figure S1).

The concept of using composition-graded nanobursa meshes is demonstrated by modeling catalytic reactions of hydrogen peroxide, H_2O_2, on the surfaces of the four metals used in this study: Pd, Co, Ag, and Pt. One of the most promising solutions for developing transformative technologies that eliminate hazardous byproducts and energy-inefficient processes for sustainable selective hydrocarbon oxidation, including propylene oxide production from propylene[25], is catalytic oxidation with H_2O_2, which can be synthesized in situ from H_2 and O_2.[26, 27] The challenge, however, is that catalysts, such as Pd and Pt nanoparticles, which are effective in catalyzing H_2O_2 formation, also catalyze its decomposition.

Table 1. Reaction energies for catalytic surfaces obtained with DFT calculations, kJ/mol

Reaction / Surface	Pd	Co	Ag	Pt
$H_2O_2 + * = H_2O_2*$ adsorption, Figure S3a	-55	N/A	-41	-61
$H_2O_2* + * = 2OH*$ decomposition leading to water formation in the presence of hydrogen, Figure S3b	-191	-434	-219	-169
$H_2O_2* + * = OOH* + H*$ decomposition leading to oxygen formation in the absence of hydrogen, Step 1, Figure S3c	7	-115	64	21
$OOH* + * = OO* + H*$ decomposition leading to oxygen formation in the absence of hydrogen, Step 2, Figure S3d	-9	-94	106	27

[1]* denotes a catalytic active site on a metal surface

[2]For Co, molecular hydrogen peroxide is not stable on the surface, and the reaction energies are calculated using hydrogen peroxide prior to adsorption: $H_2O_2 + 2* = 2OH*$ and $H_2O_2 + 2* = OOH* + H*$.

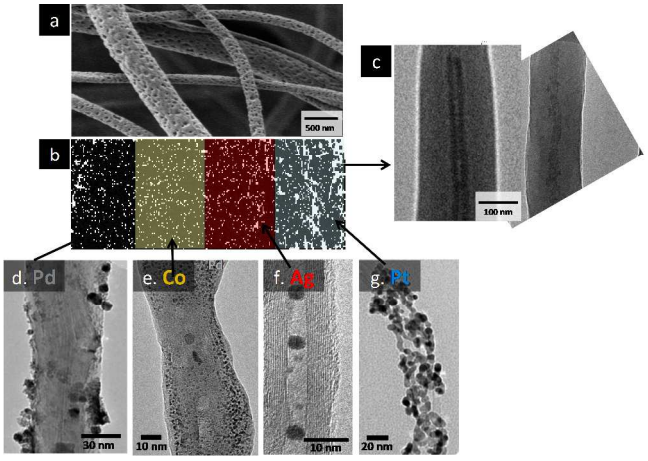

Fig. 2 SEM and TEM micrographs of components of a graded nanofibrous (nanobursa) mesh: (a) Porous polymer nanofibers, (b) Electrospun mesh, (c) Polymer nanofibers encapsulating Co-functionalized CNTs, (d) CNT functionalized with Pd, (e) CNT functionalized with Co, (f) CNT functionalized with Ag and, (g) CNT functionalized with Pt nanoparticles.

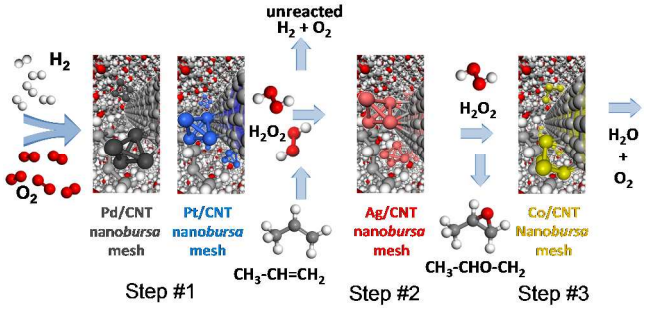

Fig. 3 Concept of consecutive catalytic reactions using a composition graded nanofibrous (nanobursa) mesh: (1) H_2O_2 formation from H_2 and O_2 over Pd and Pt, (2) propylene oxide formation from propylene and H_2O_2 over Ag, and (3) H_2O_2 decomposition over Co.

Catalytic decomposition of H_2O_2 can proceed through two pathways: (1) O-O bond cleavage and (2) O-H bond cleavage. Experimental evaluation of simultaneous H_2O_2 formation and decomposition through these two competing pathways is challenging. Instead, quantum chemical calculations based on density functional theory (DFT) have been used successfully for modeling these reactions.[28, 29]

Our DFT computational results were obtained with metal surface models constructed similarly to Pt and Co catalyst models reported earlier.[16-18] The computational results, which are summarized in Table 1 and Figures S2-S3, indicate that the first decomposition pathway through O-O bond cleavage and formation of two surface OH groups is highly exothermic and, therefore, thermodynamically favorable on Pd, Co, Ag, and Pt (Table 1). As a result, H_2O_2 decomposition in the presence of H_2 is expected to be facile on all the evaluated metals through the O-O bond cleavage mechanism. In contrast, in the absence of H_2 when H_2O_2 decomposition must proceed only through O-H bond cleavage, the formation of OOH and H surface species becomes thermodynamically unfavorable on Pt, Pd and, especially, Ag. Therefore, undesirable H_2O_2 decomposition over these metals can be suppressed by eliminating H_2 from the reacting mixture, i.e., by separating H_2O_2 formation from its utilization in selective hydrocarbon oxidation over consecutive layers of graded nanobursa meshes, as illustrated in Figure 3. In step #1, graded nanobursa mesh layers with Pt or Pd generate H_2O_2 in situ from H_2 and O_2. In order to minimize wasteful H_2O_2 decomposition, any unreacted H_2 is separated to allow oxidation of propylene to propylene oxide to take place efficiently in the absence of H_2 over a nanobursa mesh with Ag (step #2). In step #3, propylene oxide is separated, and a nanobursa mesh with Co is used for efficient decomposition of any remaining unreacted H_2O_2.

In summary, graded nanofibrous meshes fabricated with the newly developed hybrid process that combines twin-screw extrusion and electrospinning offer exciting new opportunities for catalytic technologies as well as for engineering of filters and sensors. For example, catalytic systems can be developed for the petroleum refining and chemical industries using graded nanobursa meshes where the reactants are first pretreated to remove impurities over a layer with Pt nanoparticles and then are reacted with improved activity and selectivity, due to a lack of impurities, over a layer with Ag nanoparticles. Alternatively, the concentration of catalytic Pt or other metal nanoparticles can be gradually increased in consecutive layers in order to better control reaction rates in fixed bed flow reactors. In the initial layer, the concentration of Pt should be small to prevent excessive reaction rates when the reactor feed is mostly pure reactants. In the consecutive catalyst layers along the reactor bed, the concentration of Pt should be progressively higher in order to maintain adequate reaction rates as the concentrations of the reactants decrease. In sensing applications, different layers, each with a separate type of sensing element, using different metal nanoparticles, can selectively respond to different chemicals, thus significantly expanding the utility of such sensors. Similarly in environmental sorption applications, each functionalized layer of the nanobursa mesh can selectively target a specific pollutant for more effective overall purification. The choices of the polymer, additives and their concentration distributions can be tailored in order to address permeability and stability issues and, thus, broaden the range of applications of such graded nanobursa meshes.

Acknowledgements

The DFT calculations and microscopy measurements were partially supported by the National Science Foundation under grants CBET-1264453 and DMR-0922522. The Materials Studio software was used under a collaborative research license from Accelrys Software, Inc. in San Diego, California, USA.

Notes and references

1. Y. Dzenis, *Science*, 2004, **304**, 1917-1919.
2. H. Ye, H. Lam, N. Titchenal, Y. Gogotsi and F. Ko, *Appl. Phys. Lett.*, 2004, **85**, 1775-1777.
3. L. Lu and W. Chen, *Nanoscale*, 2011, **3**, 2412-2420.
4. J. Doshi and D. H. Reneker, *J. Electrost.*, 1995, **35**, 151-160.
5. A. L. Yarin, S. Koombhongse and D. H. Reneker, *J. Appl. Phys.*, 2001, **90**, 4836-4846.
6. Y.-f. Wang, H.-f. Guo and D.-j. Ying, *J. Biomed. Mater. Res., Part B*, 2013, **101**, 1359-1366.
7. C. Erisken, D. M. Kalyon, H. Wang, C. Örnek-Ballanco and J. Xu, *Tissue Eng. A*, 2011, **17**, 1239-1252.
8. C. K. Poh, S. H. Lim, H. Pan, J. Lin and J. Y. Lee, *J. Power Sources*, 2008, **176**, 70-75.
9. X. Zhang, W. Jiang, D. Song, Y. Liu, J. Geng and F. Li, *Propellants, Explos., Pyrotech.*, 2009, **34**, 151-154.
10. C. Gao, W. Li, Y. Z. Jin and H. Kong, *Nanotechnology*, 2006, **17**, 2882-2890.
11. N. Karousis, G. E. Tsotsou, F. Evangelista, P. Rudolf, N. Ragoussis and N. Tagmatarchis, *J. Phys. Chem. C*, 2008, **112**, 13463-13469.
12. Z. Liu, X. Lin, J. Y. Lee, W. Zhang, M. Han and L. M. Gan, *Langmuir*, 2002, **18**, 4054-4060.
13. P. R. Somani, S. P. Somani and M. Umeno, *Appl. Phys. Lett.*, 2008, **93**.
14. D. R. Kauffman, D. C. Sorescu, D. P. Schofield, B. L. Allen, K. D. Jordan and A. Star, *Nano Letters*, 2010, **10**, 958-963.
15. P. Singh, M. V. Kulkarni, S. P. Gokhale, S. H. Chikkali and C. V. Kulkarni, *Appl. Surf. Sci.*, 2012, **258**, 3405-3409.

16. J. Gao, H. Zhao, X. Yang, B. E. Koel and S. G. Podkolzin, *Angew. Chem., Int. Ed.*, 2014, **53**, 3641-3644.
17. S. G. Podkolzin, G. B. Fitzgerald and B. Koel, E., in *Applications of Molecular Modeling to Challenges in Clean Energy*, American Chemical Society, 2013, vol. 1133, ch. 9, pp. 153-176.
18. J. Gao, H. Zhao, X. Yang, B. E. Koel and S. G. Podkolzin, *ACS Catal.*, 2013, **3**, 1149-1153.
19. R. I. Masel, *Principles of adsorption and reaction on solid surfaces*, Wiley, 1996.
20. H. M. Torres Galvis, J. H. Bitter, C. B. Khare, M. Ruitenbeek, A. I. Dugulan and K. P. de Jong, *Science*, 2012, **335**, 835-838.
21. A. W. A. M. van der Heijden, S. G. Podkolzin, M. E. Jones, J. H. Bitter and B. M. Weckhuysen, *Angew. Chem., Int. Ed.*, 2008, **47**, 5002-5004.
22. J. M. Planeix, N. Coustel, B. Coq, V. Brotons, P. S. Kumbhar, R. Dutartre, P. Geneste, P. Bernier and P. M. Ajayan, *J. Am. Chem. Soc.*, 1994, **116**, 7935-7936.
23. X. Pan, Z. Fan, W. Chen, Y. Ding, H. Luo and X. Bao, *Nat. Mater.*, 2007, **6**, 507-511.
24. S. Senturk-Ozer, D. Ward, H. Gevgilili and D. M. Kalyon, *Polym. Eng. Sci.*, 2013, **53**, 1463-1474.
25. T. A. Nijhuis, M. Makkee, J. A. Moulijn and B. M. Weckhuysen, *Ind. Eng. Chem. Res.*, 2006, **45**, 3447-3459.
26. M. D. Hughes, Y. J. Xu, P. Jenkins, P. McMorn, P. Landon, D. I. Enache, A. F. Carley, G. A. Attard, G. J. Hutchings, F. King, E. H. Stitt, P. Johnston, K. Griffin and C. J. Kiely, *Nature*, 2005, **437**, 1132-1135.
27. J. K. Edwards, B. Solsona, E. Ntainjua N, A. F. Carley, A. A. Herzing, C. J. Kiely and G. J. Hutchings, *Science*, 2009, **323**, 1037-1041.
28. R. Todorovic and R. J. Meyer, *Catal. Today*, 2011, **160**, 242-248.
29. D. C. Ford, A. U. Nilekar, Y. Xu and M. Mavrikakis, *Surf. Sci.*, 2010, **604**, 1565-1575.